RAPID COMMUNICATIONS

PHYSICAL REVIEW A VOLUME 48, NUMBER 1 JULY 1993

Field-induced resonances in four-wave mixing

Nadav Horesh and Yehiam Prior*
Department of Chemical Physics, Weizmann Institute of Science, Rehovot, Israel 76100
(Received 17 March 1993)

An experimental observation of field-induced resonances in four-wave mixing is reported. In experiments on Na vapor near the D lines, when the input fields are strong, new resonances appear, confirming recent theoretical predictions based on a nonperturbative approach to wave-mixing processes. The analogy to and differences from the pressure-induced extra resonances are discussed.

PACS number(s): 42.65.Hw

The analysis of nonlinear laser spectroscopy in terms of the nonlinear susceptibilities, developed by Bloembergen [1] and co-workers in the early 1960s, has been very powerful in handling the vast majority of experimental situations. In this approach, the response of a medium to laser excitation is expanded in a power series of the induced polarization, usually neglecting all orders higher than the first nonvanishing one. The well known 48-term expression for the third-order susceptibility, $\chi^{(3)}$, was derived by Bloembergen [2] from perturbation theory with phenomenological decay rates for each element of the density matrix. The pressure-induced extra resonances (PIER4) in four-wave mixing (FWM), predicted theoretically and observed experimentally in an atomic-vapor system [3], provided a striking demonstration of the power of the perturbative approach, when proper treatment of time ordering is maintained.

The PIER4 resonances were shown to be the result of cancellation of destructive interferences between terms in the expression for the third-order nonlinear susceptibility $\chi^{(3)}$, brought about by the proper dephasing effect of collisions. Other mechanisms, such as laser-field fluctuations [4], spontaneous emission [5], or radiative relaxation [6] were also shown to give rise to extra resonances. The common theme to all these processes is that they may be regarded as "effective dephasing." The topic of extra resonances was recently reviewed in two extensive papers [7].

In higher-order perturbation calculations [8], the number of terms that should be called "extra" rises very rapidly, and above fifth order most resonances are extra. Strong fields, however, where a field is strong if its Rabi frequency is large compared to its detuning and all other rates involved in the relevant transition, are not described properly by perturbative approaches, even when used in high order. Several strong-field FWM studies were reported: Ducloy *et al.* [9] studied optical phase conjugation line shapes, and the propagation of intense laser beams building a Raman mode between the dressed states was studies by Boyd *et al.* [10]. Dick and Höchstrasser [11] have theoretically analyzed nonlinear optical interactions with one strong field, and in their calculations they observed (but did not analyze in detail) power-induced resonances and noted their relation to PIER4. Friedman and Wilson Gordon [12] have also theoretically analyzed several strong-field configurations, and discussed field-induced resonances. Very recently, the approach of radiative renormalization was applied [13], and analytic expressions were derived for the nonlinear response of a medium to near-resonant strong fields.

In two theoretical papers [14, 15], we have extended the analysis of Ref. [11], and presented a nonperturbative theory for the treatment of FWM, where by a unitary transformation to an effective rotating frame the fast time dependencies are removed for all three input fields. The transformation is analogous to the rotating-wave approximation done routinely for a single field interacting with a two-level system, and it enables the handling of situations where perturbation calculations fail and all fields are strong. In that work it was shown that when strong fields are applied near resonance, new features appear, and under the proper conditions, field-induced resonances (FIRE) may be observed.

In the present Rapid Communication the experimental investigation of the interaction of strong resonant fields with a multilevel atomic system is described. We demonstrate the generation of the field-induced resonances, and provide an intuitive interpretation in terms of the dressed atom terminology [16]. The experiments were performed in sodium vapor near the D lines, and the leading diagram for FWM in Na is depicted in Fig. 1. Hyperfine and Zeeman degeneracies are ignored in the present treat-

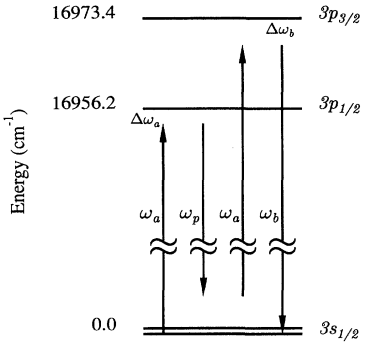

FIG. 1. The dominant energy-level diagram for the four-wave-mixing experiments in Na vapor. The pump beam at $\Delta\omega_a$ interacts with the D_1 line, while the probe at $\Delta\omega_b$ interacts nonresonantly with the D_2 transition. The same pump laser supplies the third frequency, but, being far from any resonance, it is taken as weak.

ment. Laser frequencies are denoted by their detuning:

$$\Delta\omega_a \equiv \omega_a - \omega_{D_1},$$
$$\Delta\omega_b \equiv \omega_b - \omega_{D_2},$$

where ω_a, ω_b are the laser frequencies, $\omega_{D_1} = \omega_{3s_{1/2}\to 3p_{1/2}}$, $\omega_{D_2} = \omega_{3s_{1/2}\to 3p_{3/2}}$, and all spectra shown in this paper are the total FWM intensity versus the probe detuning. The strong pump at ω_a (on or off resonance) splits the D_1 transition, inducing Rabi splitting (or ac Stark effect). Unlike the simple two-level case, where all fields are coupled to the same transition, within a four-level system, the FWM process connects (via a two-photon process involving $-\omega_b + \omega_a$) the split $3p_{1/2}$ level to the $3p_{3/2}$ level. The strong-field theory predicts that when a strong pump beam (laser frequency ω_a and Rabi frequency Ω_a) is fixed near the D_1 line and a weak probe beam is scanned around both D lines, resonance enhancement of the FWM signal should occur: (a) for the trivial case of the ordinary resonances, when the frequencies ω_b and ω_p nearly match an atomic transition frequency from the ground state ($\omega_p = 2\omega_a - \omega_b$), (b) under the conditions of the FIRE, i.e, a degenerate resonance near $\omega_b = \omega_a$ and nondegenerate resonances near $\omega_b - \omega_a = |\omega_{D_1} - \omega_{D_2}|$. Exact resonance conditions depend on the field strengths, and are given in Eq. (1) below.

The theoretical spectra presented here are all based on calculations done by the methods described in Ref. [15]. The experimental system consists of two dye lasers (Lambda Physik, model 3002) pumped by a XeCl excimer laser (Lambda Physik model 203), providing the pump beam at frequency ω_a and the probe at frequency ω_b. Each dye laser pulse is 25 ns long, and its nominal spectral full width at half maximum is 0.2 cm^{-1}, which is an average over many pulses. The spectral width of a single laser pulse, however, is much narrower, as we verified by independent measurements of the coherence length. Thus, for each nominal pump and probe frequencies, we calculate the response for a monochromatic field, and average for a distribution of frequencies. This averaging procedure provides a much more reliable interpretation of the observed spectra [17].

The laser beams intersect in a low density sodium vapor cell in a three-dimensional folded boxcar configuration, to produce the output beam at frequency $\omega_p = 2\omega_a - \omega_b$. In each experiment, the pump frequency is set in the vicinity of the D_1 transition, and the probe is scanned near the D_2 transition. The sodium vapor density was set such that the resonance absorption of the input laser beams and self-focusing and self-defocusing effects were negligible. In a different set of experiments, we have measured the pressure-induced resonances in the same experimental setup, and it was independently verified that under the present conditions pressure-induced effects are not observed.

For the level diagram of Fig. 1, and for $\Delta\omega_a = 7$ cm^{-1}, several resonances are expected, and appear in the measured broad probe frequency scan shown in Fig. 2. The ordinary resonances are at $\Delta\omega_b = 0$ ($\omega_b = \omega_{D_2}$), $\Delta\omega_b = -3$ cm^{-1} ($\omega_p = \omega_{D_1}$), and $\Delta\omega_b = -20.4$ cm^{-1} ($\omega_p = \omega_{D_2}$). These are ordinary resonances, observed for strong

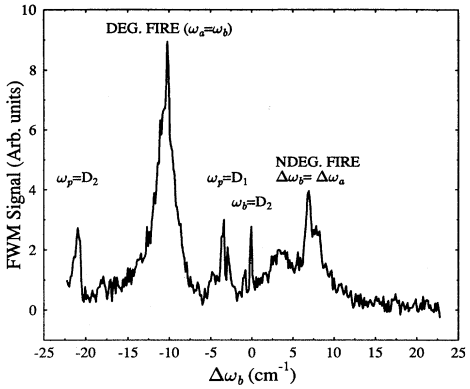

FIG. 2. A broad spectrum, showing the ordinary as well as FIRE resonances. The three ordinary resonances are at $\omega_p = \omega_{D_2}$, $\omega_p = \omega_{D_1}$, $\Delta\omega_b = 0$, and the FIRE resonances are at $\Delta\omega_b = \Delta\omega_a$ (the nondegenerate one) and at $\omega_b = \omega_a$ (the degenerate one).

as well as weak pump intensities [another ordinary resonance at $\Delta\omega_b = -17.2$ cm^{-1} ($\omega_b = \omega_{D_1}$), which comes from a different diagram is weaker and is not seen here]. In addition, two FIRE are expected at $\omega_b = \omega_a$ (the degenerate resonance) and at $\Delta\omega_b = 7$ cm^{-1} (at this frequency $\Delta\omega_a = \Delta\omega_b$ or $\omega_b - \omega_a = 17.2$ cm^{-1}—the $3p_{3/2}$-$3p_{1/2}$ frequency gap), and are clearly seen [18]. If the intensity of the pump beam is significantly reduced, the field-induced resonances disappear. In Fig. 3 a narrower scan around the resonance position for $\Delta\omega_a = 2$ cm^{-1} is shown. At relatively lower pump power (a) the ordinary resonance, even though it is power split, is still the only resonance, while at higher power (b) the ordinary resonance is saturated and the dominant feature is that of the FIRE resonance. Unlike ordinary resonances, where the power dependence of the peak intensity provides information about the order of the interaction, this is not the case for FIRE. Since FIRE is a strong-field phenomenon, the laser power dependence is complicated, and goes through several different regimes, and will not be discussed here

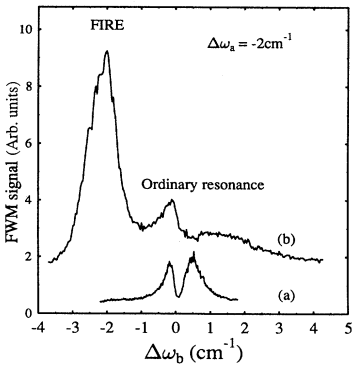

FIG. 3. A narrow scan around the FIRE position at (a) low pump laser power and (b) at high pump power, depicting the laser-field intensity as the origin of the FIRE resonance. For increasing pump power, the ordinary resonance further saturates while the FIRE resonance grows.

[17]. Figure 3, however, provides a clear demonstration of the origin of the effect, as both scans were taken at identical pressures and temperatures, and pressure effects cannot give rise to the observed resonance.

In Fig. 4 the evolution of the ordinary and FIRE resonances is depicted. Each spectrum in Fig. 4 is measured for a fixed $\Delta\omega_a$ (=0, 1, and 2 cm^{-1}). The pump beam power is set to 10^6 W/cm^2, and the probe's to 10^2 W/cm^2. As the pump is detuned from resonance, the sidebands are shifted and their amplitudes change, such that one band converges toward $\Delta\omega_b = 0$ and its amplitude increases, and the other converges toward $\Delta\omega_b = \Delta\omega_a$ and its amplitude decreases. The FIRE resonances may be intuitively understood in terms of the evolution of dressed states. The strong pump dresses the D_1 transition, creating the two Rabi sidebands. For on-resonance excitation ($\Delta\omega_a = 0$) the two dressed states are equivalent. As the detuning $\Delta\omega_a$ increases (ω_a below resonance), the lower of the two dressed states becomes "ground-state-like" while the upper one maintains the character of the excited state. Thus, one dressed state transforms into the ordinary resonance, while the other gives rise to the FIRE resonance. Note that upon detuning the pump away from resonance [$\Delta\omega_a = 0$ in Fig. 4(a) to $\Delta\omega_a = 2$ cm^{-1} in Fig. 4(c)] the actual magnitude of the ordinary resonance increases. This seemingly surprising result is also explained in terms of the dressed state model. Even though ω_a is detuned, the peaks are observed when ω_b is on resonance with a dressed state. The fact that the ordinary resonance captures the ground-state character boosts its intensity in comparison to the FIRE resonance. In the calculation of the theoretical spectra we used the known experimental values for the laser frequencies, detunings, pump-to-probe intensity ratio, and laser linewidth (as discussed above). The value of the Rabi frequency Ω was extracted from the splitting of the lines, and is the same for all spectra shown. When strong probe beam power is used, deviations from the Kramers Krönig relations between the real and imaginary parts of the induced polarization are observed, which were taken in Ref. [15] as one of the signs for the passage to the strong probe regime. For a probe which is comparable to the pump, the two sidebands lose their separate identities, acquiring properties that reflect their common origin. This case is discussed elsewhere [17].

The positions of the sidebands can be extracted from a series of measurements like the ones in Fig. 4. The peak frequencies are described by the equation

$$\Delta\omega_{b1,2} = \tfrac{1}{2}\Delta\omega_a \pm [(\tfrac{1}{2}\Delta\omega_a)^2 + \Omega_a^2]^{1/2} \quad (1)$$

which is the Rabi splitting of two levels acted upon by a strong monochromatic field. This dependence is depicted in Fig. 5, where the theoretical curve is the expression in Eq. (1), with the Rabi frequency $\Omega = 0.9$ cm^{-1}. The very good agreement of the observed and predicted peak positions completes the identification of the two resonances as resulting from the states dressed by Ω_a. Another very interesting and general result may be observed in Fig. 4: the experiments are performed with pulses which cover (in time and space) intensities ranging from zero to the maximum power at the peak of the pulse. The theoretical spectrum, on the other hand, is calculated in the steady-state limit for a fixed input power. Thus, the variable intensity of the pulse is expected to have an averaging effect, and the calculated spectra cannot fully describe the observed ones. Note, however, that the agreement between experiment and theory in Fig. 4(c) is much better than in Fig. 4(a). For $\Delta\omega_a = 0$ the splitting between the two Rabi sidebands depends on the pump intensity, and covers the range from no splitting at all to the maximal splitting. A laser pulse covers the entire range of intensities, and therefore the resonance lines are much broader. For a detuned pump laser ($\Delta\omega_a = 2$ cm^{-1}), the

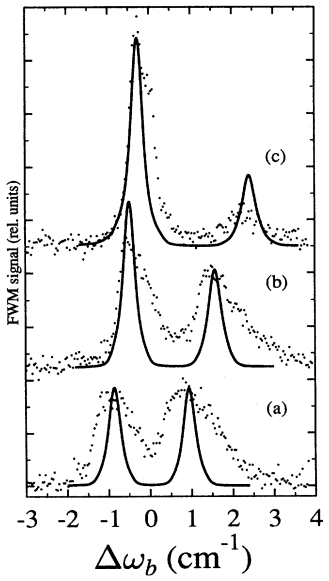

FIG. 4. The transitions from the symmetric Rabi pair to the ordinary and FIRE resonances. The three experimental spectra (points) were taken for the given values of $\Delta\omega_a$, and the theory (solid line) was calculated as discussed in the text. Note that for $\Delta\omega_a = 2$ cm^{-1} the FIRE resonance is fully developed.

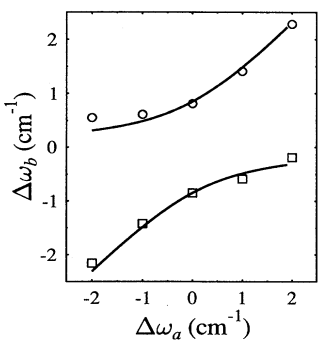

FIG. 5. The dependence of the frequency $\Delta\omega_b$ at the peak of the Rabi sidebands on the frequency $\Delta\omega_a$. The theoretical line is a fit to Eq. (1).

generalized Rabi frequency is determined mostly by the detuning ($\Omega_a < \Delta\omega_a$), its dependence on the pump laser intensity is much reduced, and the width become narrower, in better agreement with the calculated spectra.

In conclusion, the existence of the field-induced resonances was demonstrated experimentally, in good agreement with the detailed predictions of the strong-field theory of four-wave mixing. These resonances evolve from the dressed states, and their peak position, amplitude, and dependence on the exciting lasers parameters are explained. The analogy with PIER4 is very suggestive, but the differences are significant. While the existence of PIER4 (and other dephasing-induced resonances [7]) requires an effective dephasing mechanism, these new resonances are an inherent result of the strong field, and would appear even in the absence of any dephasing processes (like collisions). In our initial calculations [14] (performed in the wave-function formalism) population decay was included as phenomenological $T1$ relaxation rates (to account for spontaneous emission) but dephasing was not introduced, and the FIRE resonances were shown to result directly from the strong fields. For a pump pulse detuned far from resonance, the spectral signatures of FIRE and of PIER4 are similar, but this is where the similarity starts and ends. A PIER4 resonance does not require strong fields, and its spectral position depends only on laser detunings whereas for FIRE, strong fields are required, and therefore the spectrum depends both on detuning *and* laser power. Figures 4 and 5 demonstrate this point, and provide a clear direct way to distinguish between the two families of resonances. In any four-wave-mixing experiment where strong laser fields are applied on or near resonance, these resonances should be observable. Since many atomic and molecular transitions have a strong oscillator strength, very often a resonant laser field reaches saturating intensities. In these cases the perturbative approach does not fully describe the experimental results, and a strong-field approach should be used. In particular, for strong saturating fields, the extraction of information such as the line shape, linewidth, or peak height of a resonance line will depend very strongly on the theoretical model used.

We gratefully acknowledge useful discussions with A. M. Levine, W. M. Schreiber, N. Chencinski, A. N. Weiszman, and O. Kinrot. The work was partially supported by a grant from the U.S.-Israel Binational Science Foundation.

---

* FAX: 972-8-344126;
electronic address: CFPRIOR@WEIZMANN.AC.IL

[1] N. Bloembergen, *Nonlinear Optics* (Wiley, New York, 1965).

[2] N. Bloembergen, H. Lotem, and R. T. Lynch, Jr., Indian J. Pure Appl. Phys. **16**, 151 (1978); Y. Prior, IEEE J. Quantum Electron. **QE-20**, 37 (1984).

[3] Y. Prior, A. R. Bogdan, M. Dagenais, and N. Bloembergen, Phys. Rev. Lett. **46**, 111 (1982).

[4] A. G. Kofman, A. M. Levine, and Y. Prior, Phys. Rev. A **237**, 1248 (1988).

[5] G. S. Agarwal and P. Nayak, J. Opt. Soc. Am. **B1**, 164 (1984).

[6] G. Grynberg and M. Pinard, Europhys. Lett. **1**, 129 (1986).

[7] Theoretical as well as experimental background to the field of the extra resonances may be found in two reviews: L. Rothberg, in *Progress in Optics*, edited by E. Wolf (North-Holland, Amsterdam, 1987), Vol. 24, p. 40; G. S. Agarwal, Adv. Atom Mol. Opt. Phys. **29**, 113 (1992).

[8] R. Trebino, Phys. Rev. A **38**, 2921 (1988).

[9] M. Ducloy and D. Bloch, Opt. Commun. **47**, 351 (1983).

[10] R. W. Boyd, M. G. Raymer, P. Narum, and D. J. Harter, Phys. Rev. A **24**, 411 (1981).

[11] B. Dick and R. M. Höchstrasser, J. Phys. **75**, 133 (1983).

[12] H. Friedman and A. Wilson Gordon, Phys. Rev. A **36**, 1333 (1987), and references therein.

[13] O. Blum, T. K. Gustafson and P. L. Kelley (unpublished).

[14] A. M. Levine, N. Chencinski, W. M. Schreiber, A. N. Weiszmann, and Y. Prior, Phys. Rev. A **35**, 2550 (1987).

[15] N. Chencinsky, W. M. Schreiber, A. M. Levine, and Y. Prior, Phys. Rev. A **42**, 2839 (1990).

[16] C. Cohen-Tannoudji and S. Reynaud, J. Phys. B **10**, 345 (1977); **10**, 365 (1977).

[17] N. Horesh and Y. Prior (unpublished).

[18] A third FIRE resonance at $\omega_a - \omega_{D_2} = \omega_b - \omega_{D_1}$ stemming from a different diagram is predicted to be extremely weak, and is outside the range of the scan.